How to cite: *Angew. Chem. Int. Ed.* **2024**, *63*, e202315850
doi.org/10.1002/anie.202315850

Biosynthesis

Trapping of a Polyketide Synthase Module after C–C Bond Formation Reveals Transient Acyl Carrier Domain Interactions

Maria Dell, Mai Anh Tran, Michael J. Capper, Srividhya Sundaram, Jonas Fiedler, Jesko Koehnke, Ute A. Hellmich,* and Christian Hertweck**

Abstract: Modular polyketide synthases (PKSs) are giant assembly lines that produce an impressive range of biologically active compounds. However, our understanding of the structural dynamics of these megasynthases, specifically the delivery of acyl carrier protein (ACP)-bound building blocks to the catalytic site of the ketosynthase (KS) domain, remains severely limited. Using a multipronged structural approach, we report details of the inter-domain interactions after C–C bond formation in a chain-branching module of the rhizoxin PKS. Mechanism-based crosslinking of an engineered module was achieved using a synthetic substrate surrogate that serves as a Michael acceptor. The crosslinked protein allowed us to identify an asymmetric state of the dimeric protein complex upon C–C bond formation by cryo-electron microscopy (cryo-EM). The possible existence of two ACP binding sites, one of them a potential "parking position" for substrate loading, was also indicated by AlphaFold2 predictions. NMR spectroscopy showed that a transient complex is formed in solution, independent of the linker domains, and photochemical crosslinking/mass spectrometry of the standalone domains allowed us to pinpoint the interdomain interaction sites. The structural insights into a branching PKS module arrested after C–C bond formation allows a better understanding of domain dynamics and provides valuable information for the rational design of modular assembly lines.

Introduction

A wealth of complex, ecologically and pharmacologically important polyketides are produced by multimodular polyketide synthases (PKSs).[1] These megasynthases typically promote the assembly and processing of building blocks in a unidirectional way reminiscent of automated assembly lines. Ketosynthase (KS) domains act as the driving forces. Using activated acyl groups and malonyl units loaded onto acyl carrier proteins (ACPs) by acyl transferases (ATs), the KS domains typically catalyze Claisen condensations to construct the polyketide carbon backbone.[2] The AT domain may act *in trans* as a freestanding enzyme (*trans*-AT PKS)[3] or as an integral part of the module (*cis*-AT PKS).[4] Irrespective of the type of PKS involved, the ACP-bound condensation products, β-keto thioester intermediates, may undergo optional β-keto-processing by ketoreductase (KR), dehydratase (DH), and enoylreductase (ER) domains before they are delivered to the next module.[1] The highly programmed nature of multimodular PKSs has inspired synthetic biology approaches to design molecular assembly lines that produce tailor-made polyketides for medical, agricultural and industrial applications.[5]

A vast range of genetic and biochemical studies laid the foundation to decipher the specificities and functions of these intricate systems.[6] However, a prerequisite to the rational engineering of functional constructs is an in-depth understanding of the structural basis of the biosynthetic programs and structural dynamics of modular PKSs.[5a,7] Due to the high intrinsic flexibility of PKS modules,[8] structure elucidation with conventional methods (X-ray diffraction

[*] Dr. M. Dell, Dr. S. Sundaram, J. Fiedler, Prof. Dr. C. Hertweck
Department of Biomolecular Chemistry, Leibniz Institute for Natural Product Research and Infection Biology (HKI)
07745 Jena (Germany)
E-mail: christian.hertweck@leibniz-hki.de

Dr. M. A. Tran, Prof. Dr. U. A. Hellmich
Institute of Organic Chemistry and Macromolecular Chemistry, Friedrich Schiller University Jena
07743 Jena (Germany)
E-mail: ute.hellmich@uni-jena.de

Dr. M. J. Capper, Prof. Dr. J. Koehnke
School of Chemistry, University of Glasgow
Glasgow, G12 8QQ (UK)

Prof. Dr. J. Koehnke
Institute of Food Chemistry, Leibniz University Hannover
30167 Hannover (Germany)
E-mail: jesko.koehnke@lci.uni-hannover.de

Prof. Dr. U. A. Hellmich
Center for Biomolecular Magnetic Resonance (BMRZ), Goethe-University Frankfurt
60438 Frankfurt am Main (Germany)

Prof. Dr. U. A. Hellmich, Prof. Dr. C. Hertweck
Cluster of Excellence Balance of the Microverse, Friedrich Schiller University Jena
Jena (Germany)
and
Faculty of Biological Sciences, Friedrich Schiller University Jena
07743 Jena (Germany)

and SAXS) remains challenging. Through the structural analysis of standalone domains or didomains, exciting details of individual PKS components were revealed,[8] and nuclear magnetic resonance (NMR) spectroscopy was used to interrogate PKS domain crosstalk.[8–9] More recently, cryo-electron microscopy (cryo-EM) has shed light on the architectures of PKS modules, mainly showing parts of *cis*-AT PKSs[10] or iterative fungal PKSs.[11] Only one *trans*-AT PKS bimodule core structure is currently available.[12] Notably, transient, reversible ACP/KS domain interactions represent the most conserved architectural concept of a PKS.[13] Yet, there is only limited insight into productive KS-ACP interactions in modular PKSs in general, and no interaction model describing the dynamics between an ACP and its KS domain in *trans*-AT PKS systems has been established to date.

Here we address this gap by capturing a productive KS-ACP interaction through the implementation of genetic and chemical modification strategies, arresting a PKS module after C–C bond formation in its catalytic cycle. The interaction between KS and ACP in solution are highly transient highlighting the difficulty assessing their interactions in solution. Intriguingly, using a multipronged approach of cryo-EM, AlphaFold2 (AF2) modelling, NMR spectroscopy and mass spectrometry (MS), we find that the ACP occupies two distinct positions on its KS module. This study thus sheds light on a crucial step of interdomain crosstalk during the central step of product formation by a megasynthase.

Results and Discussion

To gain insights into the architecture of a PKS module with productive KS-ACP interactions, we employed a specialized module of the rhizoxin (**1**) PKS (Figure 1A, B) from the endofungal bacterium *Mycetohabitans rhizoxinica*[14] that introduces a chain branch.[15] Whereas the dehydratase-like B domain merely plays a structural role,[16] the KS domain of this module catalyzes a non-canonical Michael addition of the extender unit (malonate) to an α,β-unsaturated intermediate of the polyketide chain, and a subsequent intramolecular cyclization into the pharmacophoric δ-lactone ring of **1** (Figure 1A).[16–17] We sought to exploit this reaction to trap the KS-ACP interaction by mechanism-based crosslinking. Using a synthetic substrate analogue (**2**) of the ACP-bound polyketide intermediate that lacks the hydroxy group and does not allow thioester cleavage by lactonization after the Michael addition has taken place, the chain propagation was successfully stalled. As a consequence, the ACP became covalently linked to the KS domain (Figure 1C).[15c]

Initially, we biosynthetically crosslinked the isolated KS-B didomain with a free-standing ACP domain to enable the investigation of an "arrested" PKS module.[15c] The formation of the conjugate was confirmed through a resulting shift of the protein band on an SDS-PAGE (Figure S1). However, efforts to obtain crystals of this construct were not successful. After noticing that the chemical linker was partly cleaved during the purification process (Figure S1), we turned to crosslinking the KS and ACP domains within an intact module (Figure 2A). For this purpose, we heterologously produced the full-length module (KS-B-ACP) in *Escherichia coli.* To facilitate the in vivo phosphopantetheinylation of the apo-ACP, we PCR-amplified the gene encoding the endogenous phosphopantetheinyl transferase (PPTase) from *M. rhizoxinica*[18] and cloned it downstream of the KS-B-ACP-encoding gene fragment[19] (Figure 2B, for methodological details see SI). Monitoring of the in vitro enzyme branching activity by high-performance liquid chromatography (HPLC) coupled to high-resolution mass spectrometry (HRMS) showed that the construct was fully functional (Figure 2C and Figure S2). The successful formation of an interdomain crosslink in the intact protein was verified by HPLC coupled to electron spray ionization (ESI) MS (Figure 2D).

To further increase module rigidity and to shed light on the importance of the linker length for PKS module functionality, we truncated the flexible linker between the B- and ACP domain. Using the available crystal structure of the KS-B didomain deposited in the protein data bank (PDB: 4kc5), we modeled the C-terminal ACP domain and the linker connecting it to the B-domain (Figure 2E) to design three linker deletion mutants. These lack the 30 N-

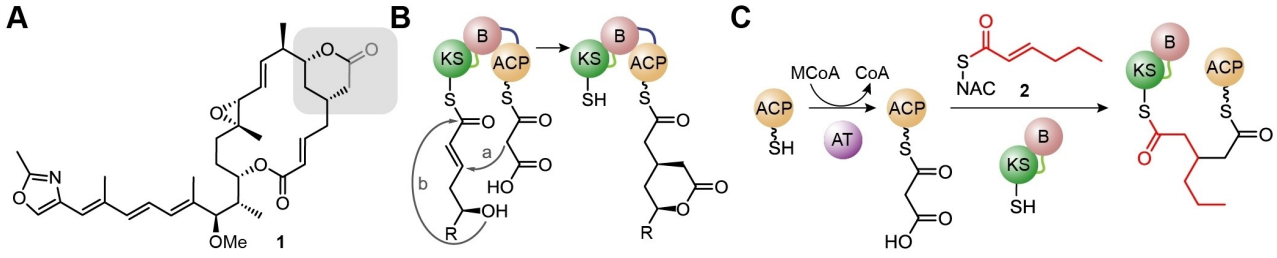

Figure 1. Polyketide branching by non-canonical conjugate addition of an extender unit. A) Structure of rhizoxin (**1**). B) A designated branching module in the RhiE subunit of the rhizoxin polyketide synthase is responsible for the formation of the δ-lactone by Michael addition (a) and lactonization (b) to the pharmacophoric δ-lactone moiety (highlighted in gray in **1**). The residue R is representative for the chain of the biosynthetic intermediate. C) Mechanism-based crosslinking strategy to tether the ACP to the KS-B didomain of the rhizoxin branching module. KS: ketosynthase; B: branching domain; ACP: acyl carrier protein; MCoA: malonyl-coenzyme A; CoA: coenzyme A; AT: acyltransferase; NAC: *N*-acetyl cysteamine.

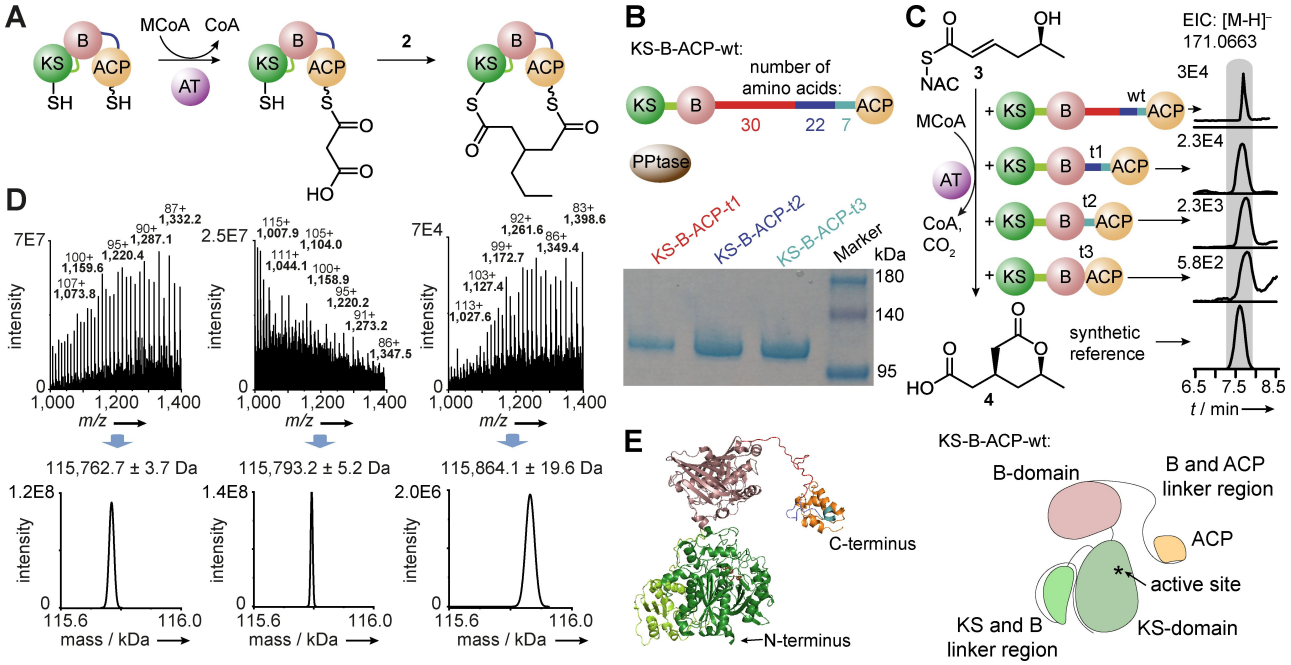

Figure 2. Biosynthetic KS-ACP crosslinking, modelling, and functional analysis of modules with truncated linkers. A) In vitro crosslinking reaction using a deoxy substrate analogue **2**. B) Heterologous expression of truncated KS-B-ACP variants with a consecutively shorter linker (KS-B-ACP-t1, -t2 and -t3, see also Figure S3). C) In vitro branching assay with the hydroxy substrate analogue (**3**) using the engineered PKS modules. D) Mass spectra of the engineered modules, and deconvoluted data. E) Using a crystal structure of KS-B (PDB: 4kc5, green/mauve), the linker and ACP domain (orange) were modelled using Phyre2server to show the putative structure of the full-length complex. Additionally, a schematic cartoon image of the PKS branching module KS-B-ACP-wt is shown to visualize the interactions that were studied. kDa: kilodalton; wt: wild type; EIC: extracted ion chromatogram.

terminal linker residues (KS-B-ACP-t1), an additional 22 amino acids (KS-B-ACP-t2) or the entire linker region, i. e. all 59 amino acids (KS-B-ACP-t3) (Figure 2B–D, and Figure S3, for more information see SI). All three constructs were successfully produced in *E. coli* and purified (Figure 2B and S4). Not surprisingly, in vitro assays showed that the removal of the entire B-ACP linker region (in KS-B-ACP-t3) reduces the activity of the module drastically, presumably because the restrained ACP cannot reach the KS active site easily anymore. It also leads to the conclusion that without a linker region, substrate delivery through the ACP to the KS domain is hampered making product formation more challenging.

In contrast, KS-B-ACP-t1 and KS-B-ACP-t2 can still transform the substrate mimic **3** into the lactone product **4** (Figure 2C and S2), i.e., the partial removal of the linker can be tolerated by the PKS module. Importantly, this type of assay monitors the ability of the ACP domain to interact with the KS-domain on-line and does not speak to the importance of the linker length for handing the substrate over to the downstream module. Based on the outcome of the functional assays and since KS-B-ACP-t1 bears the closest architectural resemblance to the native protein, we used this construct for crosslinking and further crystallization trials. To obtain biochemically crosslinked KS-B-ACP-t1, we performed the branching reaction with the deoxy substrate **2** (Figure 2A). LC-ESI-MS measurements confirmed the formation of a covalent linkage between the KS active site and ACP. We termed this arrested protein KS-B-ACP-t1*S. Diagnostic mass shifts in the spectrum of purified crosslinked KS-B-ACP-t1*S, KS-B-ACP-t1 loaded with malonate (KS-B-ACP-t1*McoA), but not native KS-B-ACP-t1, also unequivocally showed the presence of the substrate mimic as a biosynthetic linker (Figures 2D and S5—S7).

After optimization of the reaction conditions, which significantly increased the yield of KS-B-ACP-t1*S (for details, see SI) we purified the covalently linked complex by gel filtration using a fast protein liquid chromatography (FPLC) system. Although we observed an increase in stability for KS-B-ACP-t1*S compared to KS-B-ACP-wt*S during purification, KS-B-ACP-t1*S crystals diffracted only to low resolution (ca. 20 Å; data not shown). Thus, to nonetheless obtain structural information on the PKS, we turned to cryo-EM. Using the crosslinked KS-B-ACP-t1*S construct, we obtained a high-resolution cryo-EM structure with a gold-standard Fourier shell correlation (GSFSC)[20] resolution of 2.84 Å (Figure 3A and Figure S8). The cryo-EM map of the cross-linked protein clearly shows density at the KS domain active-site residue Cys3228 (Figure 3A, inset), extending towards the exterior of the protein. While the structure of the core KS-B didomain is in good agreement with the previously determined crystal structure (PDB: 4kc5),[12c] it is notable that the cryo-EM density occupied a slightly larger volume than the crystal structure. This suggests that cryo-EM, not confined by crystal packing, has

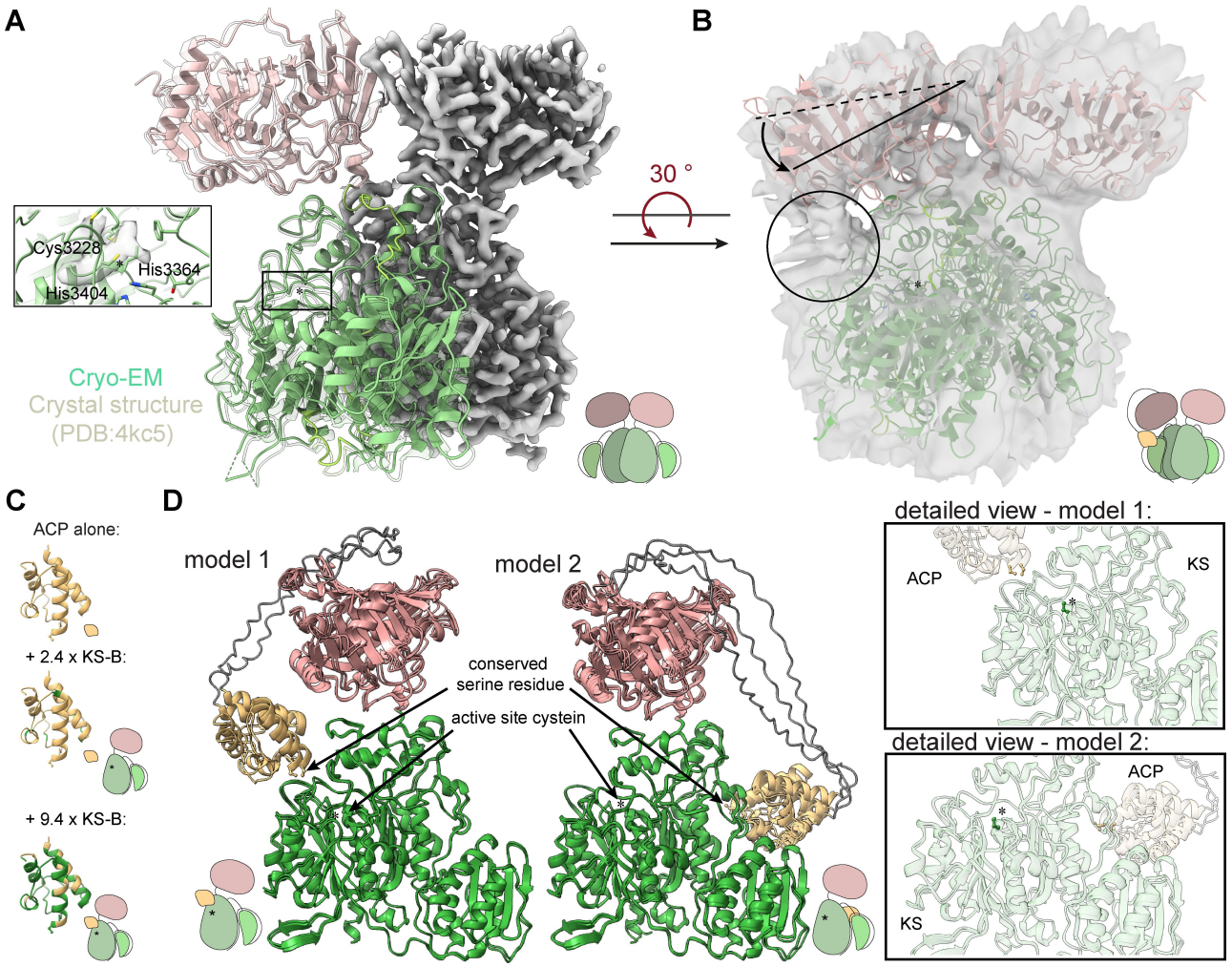

Figure 3. Structural models of rhizoxin KS-B-ACP obtained by Cryo-EM analysis and Alpha-Fold structure prediction. A) High-resolution cryo-EM structure of the RhiE module of the rhizoxin polyketide synthase, showing its KS (green) and B (mauve) domains. A previously determined crystal structure (PX, PDB: 4kc5) is shown as a gray ribbon. Inset: High-resolution image of the electron density around the covalently modified active-site Cys3228. B) Low-resolution EM volume suggesting movement of the branching domain and linking density (circle), which likely contains the highly flexible ACP domain. The dashed line represents the axis of the KS domain observed in the high-resolution structure, the arrow indicates the tilt (axis represented by solid line) in the low-resolution structure towards the active site (*). More views of the cryo-EM maps are depicted in Figure S9. C) Superposition of five AF2 KS-B-ACP models displaying two distinct binding sites of the ACP domain (yellow) on the KS-B didomain (green and mauve). Linkers are colored gray. D) NMR chemical shift mapping of ^{13}C,^{15}N-labeled RhiE-ACP (yellow) titrated with increasing molar excess of unlabeled KS indicating the transient nature of the interaction in the absence of the linker. Residues showing responses to KS addition are labeled in green (for corresponding spectra and backbone assignments, see Figure S10).

captured a native state, reflecting the dynamic nature of the PKS in solution (Figure 3A). Importantly, the particles selected for high-resolution reconstruction were refined as symmetrical dimers and did not allow us to resolve the ACP, similar to what others have seen for their respective PKS of interest.[10,12] This may either reflect the high flexibility of the ACP, or the fact that in our cryo-EM samples a significant portion of the protein had reacted with **2** (density at the KS active site Cys), but not undergone cross-linking. Nonetheless, we were able to reconstruct a lower-resolution volume from a subset of particles that showed an asymmetric conformation of the protein complex. As seen in Figure 3B, in this subset of structures, one of the B-domains was found to be tilted towards the active-site of the KS domain (Figure 3A and Figure S9 for alternative views on the structure). This orientation brings the ACP domain in close proximity to the KS domain active site. The lack of high-resolution information for this state suggests that this is a short-lived intermediate.

To probe the transient nature of the ACP-KS-B interaction and its dependence on the linker, we prepared the isolated uniformly ^{13}C,^{15}N-labeled pantetheinylated ACP for NMR spectroscopy and obtained the backbone assignment of this domain (Figures 3C and S10). Upon titration of the isotope-labeled ACP with the unlabeled KS-B didomain, severe line broadening was observed at high ratios of KS-B core to ACP domain. This suggests that the interaction between the two partners is relatively low

affinity and hence short-lived, but that the linker, or the presence of a substrate anchored to the ACP, are not requirements for complex formation per se. Importantly, NMR spectroscopy can only give information about the transient nature of the complex formation, but not the precise binding site on the KS-B module, something that was also prevented by the low resolution cryo-EM structure of the asymmetric state.

To explore the possible conformations that may have contributed to the low resolution of the asymmetric cryo-EM model and to obtain an idea about the interaction between the ACP domain and the KS-B didomain, we generated models of the structure of the full-length KS-B-ACP module. To our surprise, AF2[21] predicted two distinct ACP binding sites for the rhizoxin KS-B-ACP module (Figure 3D). In AF2 model 1, the ACP is positioned as suggested by the low-resolution cryo-EM map, placing the conserved serine residue of the ACP and the catalytic center of the KS domain ~15 Å apart. This would allow a substrate tethered to the phosphopantetheine arm to readily enter the KS active site. AF2 model 2 places the ACP on the opposite site of the KS-domain with a distance of ~40 Å from the active site (Figure 3D), too far for catalysis. It is thus tempting to speculate that this second ACP binding site represents a "parking position" for the ACP, possibly to enable efficient loading by the trans-acting AT.

To further corroborate the putative interaction sites between the KS-B didomain and ACP domain, we employed chemical crosslinking/mass spectrometry with the photo-activatable probe Sulfo-LC-SDA (**5**) (Figure 4A).[22] Undirected chemical linkage was achieved through UV irradiation of the purified KS-B-ACP-t1 in the free or cross-linked form at room temperature. After precipitation and proteolytic digest with trypsin and AspN endoproteinase, we identified the proteolytic products by HPLC-HRMS combined with a fragmentation mass spectrometry method (Figure 3E). After analyzing the data (see Figures S10—S12 and Tables S6 and S7), we visualized the crosslinks in xiNET[23] (Figure 4B) and on the structural model (Figure 4C and 4D). This experiment allowed us to identify transient protein interactions in solution that may not be captured using conventional structural biology approaches.

Interestingly, we did not detect shared crosslinks between the two samples, i. e. KS-B-ACP-t1 and KS-B-ACP-t1*S, likely corroborating the efficiency of the mechanism-based crosslink, which leads to different degrees of flexibility and protein conformations of the branching module compared to the free module. It is also possible that the conformations of biosynthetically crosslinked and free KS-B-ACP-t1 differ so much from each other that only distinct crosslinks for each state can be resolved. In the absence of the biosynthetic crosslinker, only crosslinks 1, 2 and 3 were detected (Figure 4C, S11–S13 and Tables S8–S10) that reflect intradomain KS contacts as well as between the linker region and the B-domain (in mauve). In the KS-B-ACP-t1*S sample featuring the mechanism-based crosslink of the active site, we identified three defined chemical crosslinks between KS and ACP domains (Figure 4D, crosslinks No. 4, 5 and 6, Figures S14–S16, and Table S11–S13).

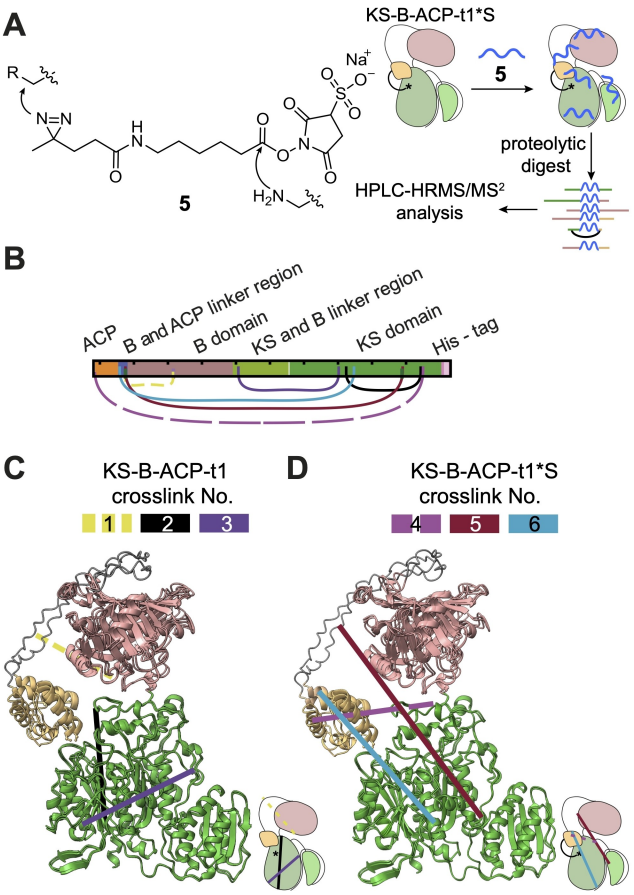

Figure 4. Workflow for crosslinking mass spectrometry of KS-B-ACP-t1*S and KS-B-ACP-t1. A) The protein was incubated with the chemical crosslinker **5** followed by proteolytic digest and analysis with HPLC-HRMS/MS². Investigating ACP binding sites by photochemical crosslinking/MS. B) Crosslinks identified and visualized using XiNet. C) Visualization of the crosslinks in the structural model of KSBACP-t1. D) Visualization of the crosslinks in the structural model of KSBACP-t1*S (see Figures S11–S16 for more details).

These reflect interactions between ACP and KS domain in the vicinity of the active site, corroborating the cryo-EM structural model and AF2 model 1 prediction. This underscores that the protein's intrinsic flexibility is reduced by the biosynthetic linker **2**, thereby enhancing the possibility to "catch" the ACP with a photochemical crosslinker. Excitingly, crosslinks 2 and 3 imply a connection between the ACP linker and the N-terminal lobe of the KS-domain (in green). This ensemble supports AF2 model 2, which we hypothesize to represent a hitherto undescribed discrete non-productive state ("parking position").

Conclusion

Deciphering protein-protein interactions within PKS modules, especially between an ACP-anchored substrate and the catalytic domains, is pivotal to understanding and engineering molecular assembly lines.[24] However, their highly flexible nature poses a significant challenge for structural

investigations.[8a,25] Since the long linker tethering the ACP domain to the catalytic modules confers flexibility, crosslinking of this domain can be used to reduce the conformational space of the PKS. Numerous crosslinkers reacting with specific side chains of the domain of interest with the ACP have been introduced[26] and yielded structures of individual domains connected to ACPs.[26a,27] Here, we aimed to harness a genuine biosynthetic linker to arrest the catalytic cycle of a PKS module and thus visualize it during C–C bond formation. The chain-branching module of the rhizoxin (**1**) PKS proved to be ideally suited for such an approach since a synthetic substrate surrogate naturally tethers the KS domain with the ACP upon enzyme-mediated Michael addition of the malonyl-ACP.

We identified two distinct positions for the ACP interacting with the KS domain, corroborated by cryo-EM, XL–MS and AF2 predictions. We propose that one of these states represents the catalytically productive state (obtained by cryo-EM and seen in AF2 model 1), while the other reflects a non-productive "parking position", likely facilitating the loading of the malonyl building block (visualized in AF2 model 2 and supported by XL–MS; Figure 5).

In the context of giant assembly lines, ACPs need to reversibly interact with different partner domains and across modules. Because of the transient nature of the ACP interactions, this carries the risk of the ACPs to diffuse away easily. To counteract this, long linkers are used to tether the ACP to the core domains. On the other hand, these extended linkers may sterically interfere with catalysis. We thus deem it likely that such a system would benefit from possessing at least one non-productive binding-site ("parking position"), to restrict the movement of the ACP when it is not needed to improve the performance of the assembly line, which may also facilitate the loading process by the *trans*-acting AT.

Interestingly, in the context of bacterial and fungal *cis*-AT PKS systems, multiple ACP binding sites of KS domains have also been reported. A structural analysis of a module of the pikromycin PKS revealed two distinct ACP binding sites, which seem to be occupied by the downstream and upstream ACPs for substrate loading or off-loading.[10b] In contrast, our study of the *rhi* PKS module shows that a singular ACP of the branching module binds to the two sites of the vicinal KS domain. Crosslinking of the erythromycin PKS module 1 with PPant derivates indicated two distinct states of the module, and in both states, the ACP binding site lies within the KS-AT cleft.[10e] In iterative fungal PKS such as the cercosporin PKS, two ACP binding sites have been identified. In contrast to the erythromycin PKS module, the ACP is assumed to sit on top of the KS-AT cleft.[11a] All of these systems differ from the *rhi* PKS module in that they harbor AT domains adjacent to the ACP. It is plausible that the absence of an AT domain within the module has an influence on the interdomain interactions of the ACP. Another structural analysis on a *trans*-AT PKS module showed that the interactions between domains are transient, however, no ACP could be visualized.[12a]

The range of methods used here to analyze structural changes in one PKS module (RhiE) shows that cryo-EM, AF2 modelling, protein NMR, and crosslinking/MS complement each other well. They allowed us to paint a fuller picture of interdomain interactions. With these results we contribute to the structural knowledge on *trans*-AT PKS modules and present protocols for the analysis of other PKS systems. In particular, this approach permitted a glance at the movement of the KS domain when interacting with the ACP during the catalytic cycle of a *trans*-AT PKS module. The combination of multiple structural methods with biosynthetic crosslinking appears to be a promising strategy to harness highly dynamic modules of megasynthases and to gain insights into productive domain interactions. We envision that such an approach will aid in elucidating the structural dynamics and interactions within more complex *trans*-AT PKS modules in the future.

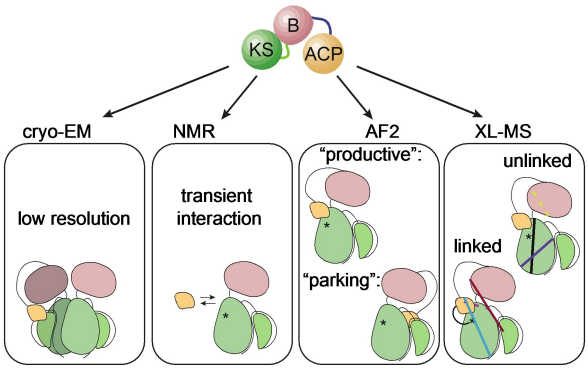

Figure 5. Summary of methods and results, showing to gain insight into the transient interactions of domains within the branching module of the *rhi* PKS.

Supporting Information

The authors have cited additional references within the Supporting Information.

Acknowledgements

We thank A. Perner and D. Braga for HPLC-HRMS measurements, G. Zocher (University of Tübingen) for initial crystallization trials, and J.-M. Harder for fruitful discussions. This work was funded by the Deutsche Forschungsgemeinschaft (DFG, German Research Foundation) under Germany's Excellence Strategy—EXC 2051—Project-ID 390713860, CRC 1127—Project-ID 239748522 (ChemBioSys) (to U.A.H. and C.H.), and Leibniz Award (to C.H.), by the European Regional Development Fund (ERDF) (MassNat) (to C.H.), and the European Research Council (ERC CoG 101002326) (to J.K.). We acknowledge the Scottish Centre for Macromolecular Imaging (SCMI) and James Streetley for assistance with cryo-EM experiments and access to instrumentation, funded by the MRC (MC_PC_17135) and SFC (H17007). U.A.H. acknowledges an instrumentation grant for a high-field NMR spectrometer

by the REACT-EU EFRE Thuringia (Recovery assistance for cohesion and the territories of Europe, ERDF, Thuringia) initiative of the European Union. Open Access funding enabled and organized by Projekt DEAL.

Conflict of Interest

The authors declare no conflict of interest.

Data Availability Statement

The data that support the findings of this study are available in the supplementary material of this article.

Keywords: Acyl Carrier Protein · Biosynthesis · Crosslinking · Electron Microscopy · Modular Polyketide Synthases

[1] a) M. A. Fischbach, C. T. Walsh, *Chem. Rev.* **2006**, *106*, 3468–3496; b) C. Hertweck, *Angew. Chem. Int. Ed.* **2009**, *48*, 4688–4716; c) J. L. Meier, M. D. Burkart, *Chem. Rev.* **2009**, *38*, 2012–2045.

[2] A. Nivina, K. P. Yuet, J. Hsu, C. Khosla, *Chem. Rev.* **2019**, *119*, 12524–12547.

[3] E. J. Helfrich, J. Piel, *Nat. Prod. Rep.* **2016**, *33*, 231–316.

[4] A. T. Keatinge-Clay, *Chem. Rev.* **2017**, *117*, 5334–5366.

[5] a) C. Hertweck, *Trends Biochem. Sci.* **2015**, *40*, 189–199; b) S. Yuzawa, J. D. Keasling, L. Katz, *J. Antibiot.* **2017**, *70*, 378–385; c) K. A. Bozhüyük, J. Micklefield, B. Wilkinson, *Curr. Opin. Microbiol.* **2019**, *51*, 88–96; d) T. Kornfuehrer, A. S. Eustaquio, *MedChemComm* **2019**, *10*, 1256–1272.

[6] a) K. J. Weissman, P. F. Leadlay, *Nat. Rev. Microbiol.* **2005**, *3*, 925–936; b) K. J. Weissman, *Nat. Prod. Rep.* **2016**, *33*, 203–230; c) M. Klaus, L. Buyachuihan, M. Grininger, *ACS Chem. Biol.* **2020**, *15*, 2422–2432; d) M. Klaus, M. Grininger, *Nat. Prod. Rep.* **2018**, *35*, 1070–1081; e) S. Kapur, B. Lowry, S. Yuzawa, S. Kenthirapalan, A. Y. Chen, D. E. Cane, C. Khosla, *Proc. Natl. Acad. Sci. USA* **2012**, *109*, 4110–4115; f) M. Jenner, S. Frank, A. Kampa, C. Kohlhaas, P. Poplau, G. S. Briggs, J. Piel, N. J. Oldham, *Angew. Chem. Int. Ed.* **2013**, *52*, 1143–1147; g) E. J. N. Helfrich, R. Ueoka, A. Dolev, M. Rust, R. A. Meoded, A. Bhushan, G. Califano, R. Costa, M. Gugger, C. Steinbeck, P. Moreno, J. Piel, *Nat. Chem. Biol.* **2019**, *15*, 813–821; h) P. D. Gerlinger, G. Angelidou, N. Paczia, T. J. Erb, *bioRxiv preprint* **2023**, 2023.2002.2016.528826.

[7] M. Klaus, M. P. Ostrowski, J. Austerjost, T. Robbins, B. Lowry, D. E. Cane, C. Khosla, *J. Biol. Chem.* **2016**, *291*, 16404–16415.

[8] a) T. Robbins, Y. C. Liu, D. E. Cane, C. Khosla, *Curr. Opin. Struct. Biol.* **2016**, *41*, 10–18; b) K. J. Weissman, *Nat. Prod. Rep.* **2015**, *32*, 436–453.

[9] a) V. Y. Alekseyev, C. W. Liu, D. E. Cane, J. D. Puglisi, C. Khosla, *Protein Sci.* **2007**, *16*, 2093–2107; b) L. K. Charkoudian, C. W. Liu, S. Capone, S. Kapur, D. E. Cane, A. Togni, D. Seebach, C. Khosla, *Protein Sci.* **2011**, *20*, 1244–1255.

[10] a) J. Davison, J. Dorival, H. Rabeharindranto, H. Mazon, B. Chagot, A. Gruez, K. J. Weissman, *Chem. Sci.* **2014**, *5*, 3081–3095; b) S. Dutta, J. R. Whicher, D. A. Hansen, W. A. Hale, J. A. Chemler, G. R. Congdon, A. R. Narayan, K. Hakansson, D. H. Sherman, J. L. Smith, G. Skiniotis, *Nature* **2014**, *510*, 512–517; c) J. R. Whicher, S. Dutta, D. A. Hansen, W. A. Hale, J. A. Chemler, A. M. Dosey, A. R. Narayan, K. Hakansson, D. H. Sherman, J. L. Smith, G. Skiniotis, *Nature* **2014**, *510*, 560–564; d) J. L. Smith, G. Skiniotis, D. H. Sherman, *Curr. Opin. Struct. Biol.* **2015**, *31*, 9–19; e) D. P. Cogan, K. Zhang, X. Li, S. Li, G. D. Pintilie, S. H. Roh, C. S. Craik, W. Chiu, C. Khosla, *Science* **2021**, *374*, 729–734; f) S. R. Bagde, I. Mathews, J. C. Fromme, C. Y. Kim, *Science* **2021**, *374*, 723–729; g) J. L. Faylo, D. W. Christianson, *J. Struct. Biol.* **2021**, *213*, 107802; h) M. S. Dickinson, T. Miyazawa, R. S. McCool, A. T. Keatinge-Clay, *Structure* **2022**, *30*, 1331–1339; i) S. K. Kim, M. S. Dickinson, J. Finer-Moore, Z. Guan, R. M. Kaake, I. Echeverria, J. Chen, E. H. Pulido, S. Sali, N. J. Krogan, O. S. Rosenberg, R. M. Stroud, *Nat. Struct. Mol. Biol.* **2023**, *30*, 296–308.

[11] a) D. A. Herbst, C. R. Huitt-Roehl, R. P. Jakob, J. M. Kravetz, P. A. Storm, J. R. Alley, C. A. Townsend, T. Maier, *Nat. Chem. Biol.* **2018**, *14*, 474–479; b) J. Wang, J. Liang, L. Chen, W. Zhang, L. Kong, C. Peng, C. Su, Y. Tang, Z. Deng, W. Z., *Nat. Commun.* **2021**, *12*, 867.

[12] a) Y. U. Tittes, D. A. Herbst, S. F. X. Martin, H. Munoz-Hernandez, R. P. Jakob, T. Maier, *Sci. Adv.* **2022**, *8*, eabo6918; b) M. Grininger, *Nat. Chem. Biol.* **2023**, *19*, 401–415.

[13] L. Buyachuihan, F. Stegemann, M. Grininger, *Angew. Chem. Int. Ed.* **2024**, *63*, e202312476.

[14] a) L. P. Partida-Martinez, C. Hertweck, *Nature* **2005**, *437*, 884–888; b) K. Scherlach, L. P. Partida-Martinez, H. D. Dahse, C. Hertweck, *J. Am. Chem. Soc.* **2006**, *128*, 11529–11536; c) K. Scherlach, B. Busch, G. Lackner, U. Paszkowski, C. Hertweck, *Angew. Chem. Int. Ed.* **2012**, *51*, 9615–9618.

[15] a) L. P. Partida-Martinez, C. Hertweck, *ChemBioChem* **2007**, *8*, 41–45; b) B. Kusebauch, B. Busch, K. Scherlach, M. Roth, C. Hertweck, *Angew. Chem. Int. Ed.* **2009**, *48*, 5001–5004; c) T. Bretschneider, J. B. Heim, D. Heine, R. Winkler, B. Busch, B. Kusebauch, T. Stehle, G. Zocher, C. Hertweck, *Nature* **2013**, *502*, 124–128.

[16] S. Sundaram, D. Heine, C. Hertweck, *Nat. Chem. Biol.* **2015**, *11*, 949–951.

[17] S. Sundaram, H. J. Kim, R. Bauer, T. Thongkongkaew, D. Heine, C. Hertweck, *Angew. Chem. Int. Ed.* **2018**, *57*, 11223–11227.

[18] G. Lackner, N. Moebius, L. P. Partida-Martinez, S. Boland, C. Hertweck, *BMC Genomics* **2011**, *12*.

[19] R. J. Cox, T. S. Hitchman, K. J. Byrom, I. Stuart, C. Findlow, J. A. Tanner, J. Crosby, T. J. Simpson, *FEBS Lett.* **1997**, *405*, 267–272.

[20] R. Henderson, A. Sali, M. L. Baker, B. Carragher, B. Devkota, K. H. Downing, E. H. Egelman, Z. Feng, J. Frank, N. Grigorieff, W. Jiang, S. J. Ludtke, O. Medalia, P. A. Penczek, P. B. Rosenthal, M. G. Rossmann, M. F. Schmid, G. F. Schröder, A. C. Steven, D. L. Stokes, J. D. Westbrook, W. Wriggers, H. Yang, J. Young, H. M. Berman, W. Chiu, G. J. Kleywegt, C. L. Lawson, *Structure* **2012**, *20*, 205–214.

[21] a) J. Jumper, R. Evans, A. Pritzel, T. Green, M. Figurnov, O. Ronneberger, K. Tunyasuvunakool, R. Bates, A. Zidek, A. Potapenko, A. Bridgland, C. Meyer, S. A. A. Kohl, A. J. Ballard, A. Cowie, B. Romera-Paredes, S. Nikolov, R. Jain, J. Adler, T. Back, S. Petersen, D. Reiman, E. Clancy, M. Zielinski, M. Steinegger, M. Pacholska, T. Berghammer, S. Bodenstein, D. Silver, O. Vinyals, A. W. Senior, K. Kavukcuoglu, P. Kohli, D. Hassabis, *Nature* **2021**, *596*, 583–589; b) M. Varadi, S. Anyango, M. Deshpande, S. Nair, C. Natassia, G. Yordanova, D. Yuan, O. Stroe, G. Wood, A. Laydon, A. Zidek, T. Green, K. Tunyasuvunakool, S. Petersen, J. Jumper, E. Clancy, R. Green, A. Vora, M. Lutfi, M. Figurnov, A. Cowie, N. Hobbs, P. Kohli, G. Kleywegt, E. Birney, D. Hassabis, S. Velankar, *Nucleic Acids Res.* **2022**, *50*, D439-D444.

[22] A. F. Gomes, F. C. Gozzo, *J. Mass Spectrom.* **2010**, *45*, 892–899.

[23] C. W. Combe, L. Fischer, J. Rappsilber, *Mol. Cell. Proteomics* **2015**, *14*, 1137–1147.
[24] a) G. J. Dodge, F. P. Maloney, J. L. Smith, *Nat. Prod. Rep.* **2018**, *35*, 1082–1096; b) E. M. Musiol-Kroll, W. Wohlleben, *Antibiotics* **2018**, *7*, 62.
[25] K. J. Weissman, *Nat. Chem. Biol.* **2015**, *11*, 660–670.
[26] a) C. Nguyen, R. W. Haushalter, D. J. Lee, P. R. Markwick, J. Bruegger, G. Caldara-Festin, K. Finzel, D. R. Jackson, F. Ishikawa, B. O'Dowd, J. A. McCammon, S. J. Opella, S. C. Tsai, M. D. Burkart, *Nature* **2014**, *505*, 427–431; b) A. S. Worthington, G. H. Hur, J. L. Meier, Q. Cheng, B. S. Moore, M. D. Burkart, *ChemBioChem* **2008**, *9*, 2096–2103; c) G. A. R. Thiele, C. P. Friedman, K. J. S. Tsai, J. Beld, C. H. Londergan, L. K. Charkoudian, *Biochemistry* **2017**, *56*, 2533–2536; dS. Konno, J. J. La Clair, M. D. Burkart, *Angew. Chem. Int. Ed.* **2018**, *57*, 17009–17013.
[27] a) A. S. Worthington, D. F. Porter, M. D. Burkart, *Org. Biomol. Chem.* **2010**, *8*, 1769–1772; b) A. Miyanaga, R. Ouchi, F. Ishikawa, E. Goto, G. Tanabe, F. Kudo, T. Eguchi, *J. Am. Chem. Soc.* **2018**, *140*, 7970–7978; c) S. Kapur, A. Worthington, Y. Tang, D. E. Cane, M. D. Burkart, C. Khosla, *Bioorg. Med. Chem. Lett.* **2008**, *18*, 3034–3038; d) M. N. Johnson, C. H. Londergan, L. K. Charkoudian, *J. Am. Chem. Soc.* **2014**, *136*, 11240–11243; e) Z. Ye, M. Bair, H. Desai, G. J. Williams, *Mol. BioSyst.* **2011**, *7*, 3152–3156.

Manuscript received: October 19, 2023
Accepted manuscript online: December 22, 2023
Version of record online: January 17, 2024